

## Optimum classical beam-position sensing

Wenhua He<sup>1,\*</sup>, Christos N. Gagatsos<sup>1,2,3</sup>, Dalziel J. Wilson<sup>1</sup>, and Saikat Guha<sup>1,4</sup>

<sup>1</sup> Wyant College of Optical Sciences, University of Arizona, Tucson, Arizona 85721, USA

<sup>2</sup> Department of Electrical and Computer Engineering, University of Arizona, Tucson, Arizona 85721, USA

<sup>3</sup> Program in Applied Mathematics, University of Arizona, Tucson, Arizona 85721, USA

<sup>4</sup> Department of Electrical and Computer Engineering, University of Maryland, College Park, Maryland 20742, USA



(Received 28 March 2024; accepted 9 September 2024; published 16 October 2024)

Beam-displacement measurements are widely used in optical sensing and communications; however, their performance is affected by numerous intrinsic and extrinsic factors, including beam profile, propagation loss, and receiver architecture. Here we present a framework for designing a classically optimal beam-displacement transceiver, using quantum estimation theory. We consider the canonical task of estimating the position of a diffraction-limited laser beam after passing through an apertured volume characterized by Fresnel-number product  $D_F$ . As a rule of thumb, higher-order Gaussian modes provide more information about beam displacement, but are more sensitive to loss. Applying quantum Fisher information, we design mode combinations that optimally leverage this trade-off, and show that a greater than tenfold improvement in precision is possible, relative to the fundamental mode, for a practically relevant  $D_F = 100$ . We also show that this improvement is realizable with a variety of practical receiver architectures. Our findings extend previous works on lossless transceivers, may have immediate impact on applications, such as atomic force microscopy and near-field optical communication, and pave the way towards globally optimal transceivers using nonclassical laser fields.

DOI: 10.1103/PhysRevApplied.22.L041004

**Introduction.** Estimating the transverse displacement of a laser beam is a key task in a broad range of commercial and scientific applications, from atomic force microscopy [1] and single-molecule tracking [2] to pointing-acquisition-tracking for free-space optical communications [3] and telescope stabilization [4]. Extensive theoretical and experimental work has been dedicated to realizing improved transceiver designs. In most of these studies, the transmitter is the fundamental Hermite-Gaussian mode,  $HG_{00}$ —both in the classical regime, where the laser is in a coherent state, and in quantum-enhanced schemes (e.g., by mixing a  $HG_{00}$  coherent state with phase-inverted  $HG_{00}$  squeezed vacuum [5–7]). Common receiver architectures include the split photodetector [5–7], lateral effect photodiode [8], and homodyne interferometers employing phase-inversion [9] or structured local oscillators [10–12].

In designing beam-position transceivers that move beyond conventional  $HG_{00}$  transmitters, a key insight is that higher-order Gaussian modes provide more information about beam position (via their high spatial frequency content) [10–13], albeit at the price of higher sensitivity to loss [14]. Transceivers employing high-order Hermite-Gaussian (HG) modes have been experimentally

studied [10–12], but only for a single higher-order mode. Classically optimal transmitters employing single higher-order HG modes have also been theoretically considered [12,13] using single parameter estimation theory [15]; however, as simplifying assumptions, both diffraction and loss in these studies were ignored.

Here, we present a framework for designing a classically optimal beam-displacement transceiver that allows for diffraction, loss, and arbitrary spatial modeshape, based on quantum estimation theory. The enabling tool for our study is quantum Fisher information (QFI) [15,16], which allows the spatial mode to be optimized, for a given laser (probe) state, over all possible receivers. Thus we are able to model the generic problem illustrated in Fig. 1(a), in which a Gaussian laser beam passes through an apertured (at the transmitter and receiver plane) volume characterized by Fresnel number product  $D_F$ . After identifying an (in general, nonunique) optimal spatial mode, the corresponding optimal receiver can then be found using classical Fisher information (CFI), a procedure that also yields a variety of options.

As a practical illustration [17–20], we confine our attention to coherent state transmitters and soft Gaussian apertures, relevant to common beam-displacement transceivers, such as the optical lever [Fig. 1(b)]. For practically relevant Fresnel-number product  $D_F < 100$  (approximately the number of HG modes that will survive

\*Contact author: whe1@arizona.edu

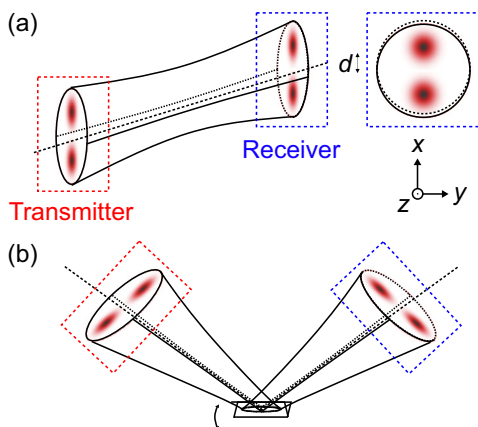


FIG. 1. (a) Transceiver model for optical beam-displacement sensing. Diffractive loss is introduced via the finite aperture of the transmitter and receiver planes, characterized by Fresnel-number product  $D_F$ . A transverse intensity pattern that maximizes the quantum Fisher information for  $D_F = 90$  is shown, assuming a coherent state with a specific energy. (b) Application to measuring the angular displacement of a reflective landscape (an optical lever measurement).

propagation through the system), we “discover” a class of two-peaked transmission modes as shown in Fig. 1(a), which represent the transverse intensity (and phase) distribution that optimally weights the trade-off between spatial derivative and diffraction loss. For  $D_F = 100$ , we predict that such a mode can outperform the HG<sub>00</sub> mode by an order of magnitude, using a variety of standard receivers.

The starting point for our analysis is an abstract Fisherian description of beam-displacement sensing. For a given Fresnel-number product  $D_F$ , transmitter mode, and receiver architecture, the CFI,  $J(d)$ , upper bounds the inverse of the minimum uncertainty with which the laser beam displacement  $d$  can be estimated [15,21]. The QFI,  $K(d)$ , is similarly related to  $d$ , but optimized over all possible receivers [15,16], and therefore a property of the transmitter state and  $D_F$  alone, viz.

$$\frac{1}{\Delta d} \leq \sqrt{J(d)} \leq \sqrt{K(d)}. \quad (1)$$

We thus adopt a mechanistic approach whereby  $K(d)$  is first optimized, yielding a subspace of optimal transmitter modes. The subset of optimal receiver architectures is then inferred by inspection, appealing to the upper bound set by Eq. (1).

To compute  $K(d)$ , we seek an expression for the multimode coherent state  $|\vec{a}(d)\rangle$  at the receiver, and use the fact that

$$K(d) = -2 \lim_{\varepsilon \rightarrow 0} \frac{\partial^2 \mathcal{F}}{\partial \varepsilon^2}, \quad (2)$$

where

$$\mathcal{F}(\varepsilon) = |\langle \vec{a}(d) | \vec{a}(d + \varepsilon) \rangle|^2, \quad (3)$$

is the fidelity [22] between states with different displacements. Following a standard approach,  $|\vec{a}(d)\rangle$  can be represented as a vector of mean values  $\{\langle \hat{q}_0 \rangle, \langle \hat{q}_1 \rangle, \dots, \langle \hat{p}_0 \rangle, \langle \hat{p}_1 \rangle, \dots\}$ , where  $\hat{a}_n, \hat{q}_n = \hat{a}_n + \hat{a}_n^\dagger$  and  $\hat{p}_n = -i(\hat{a}_n - \hat{a}_n^\dagger)$  are the annihilation, position and momentum operators for field at the receiver, decomposed into an orthonormal basis of spatial modes [23]. It thus suffices to determine the modal decomposition of the laser field at the receiver and its functional dependence on  $d$ .

We consider a coherent state of mean photon number  $N$ , and choose as our orthonormal basis the HG modes— $\Phi_n(x)\Phi_m(y)$  at the transmitter and  $\phi_n(x)\phi_m(y)$  at the receiver (Fig. 1)—as they form a singular value decomposition of the soft-aperture propagation kernel [14,24]. Noting that only  $\Phi_n(x)$  is sensitive to displacement and  $\Phi_0(y)$  is least sensitive to diffraction loss, an optimal transmitted field can be expressed as

$$\Psi(x, y) = \sqrt{N} \sum_{n=0}^{M_s-1} c_n e^{i\theta_n} \Phi_n(x) \Phi_0(y), \quad (4)$$

with expansion coefficients  $c_n, \theta_n \in \mathfrak{N}$  satisfying  $\sum_n c_n^2 = 1$ .

The beam is now allowed to propagate through the optical system, whose loss we model by placing soft Gaussian apertures of radius  $r_T$  and  $r_R$  at the transmitter and receiver, respectively, separated by a distance  $L$ . The net loss is characterized by Fresnel number product  $D_F = (kr_T r_R / 4L)^2$ , which approximates the number of HG modes that can pass through the optical system with negligible loss. If the beam undergoes a transverse displacement  $d \ll r_R$  during propagation, then the field beyond the receiver aperture can be expressed as

$$\psi(x + d, y) \approx \sqrt{N} \sum_{m,n=0}^{M_s-1} Q_{mn}(\tilde{d}) \sqrt{\eta^{n+1}} c_n e^{i\theta_n} \phi_m(x) \phi_0(y), \quad (5)$$

where

$$\eta = \frac{1 + 2D_F - \sqrt{1 + 4D_F}}{2D_F} \quad (6)$$

is the transmissivity of the HG<sub>00</sub> mode,  $Q_{mn}(\tilde{d})$  is a cross-talk matrix characterizing spatial-mode coupling, and for convenience we define the normalized displacement  $\tilde{d} \equiv d/r_R$  [24].

Equation (5) implies that for a given transmitter mode, all information about displacement is encoded in the cross-talk matrix  $Q_{mn}(\tilde{d})$ , and that information in higher-order

modes must be leveraged against transmission loss  $\eta^{n+1}$ . Our main result is to formalize this statement, viz, combining Eqs. (2)–(6) and the cross-talk matrix derived in the Supplemental Material, and noting that

$$\begin{aligned} \langle \hat{q}_m \rangle &= 2\text{Re} \left\{ \sqrt{N} \sum_{n=m-1}^{m+1} Q_{mn}(\tilde{d}) \sqrt{\eta^{n+1}} c_n e^{i\theta_n} \right\}, \\ \langle \hat{p}_m \rangle &= 2\text{Im} \left\{ \sqrt{N} \sum_{n=m-1}^{m+1} Q_{mn}(\tilde{d}) \sqrt{\eta^{n+1}} c_n e^{i\theta_n} \right\}, \end{aligned} \quad (7)$$

we arrive at the following QFI assuming  $r_T = r_R \equiv r_0$ ,

$$\begin{aligned} K(\tilde{d}) &= 16\eta N \left( \sum_{j=0}^{M_s-1} (j + (2j+1)D_F(1-\eta)) \eta^j c_j^2 \right. \\ &\quad \left. - \eta \sum_{j=0}^{M_s-3} \sqrt{4(j+1)(j+2)D_F} \eta^j c_j c_{j+2} \sin(\theta_j - \theta_{j+2}) \right), \end{aligned} \quad (8)$$

where  $M_s$  is the highest mode order allowed.

In Fig. 2, we use Eq. (8) to visualize the landscape of classically optimal spatial modes for beam-displacement sensing, and their performance as a function of the Fresnel-number product  $D_F$  of the optical system. Intuitively, larger  $D_F$  allows for a larger spatial mode support  $M_s$ , which in turn gives access to higher displacement sensitivity, using an optimal receiver. This reasoning is borne out in Figs. 2(a) and 2(b), in which the QFI per photon  $K/N$  is plotted versus  $M_s$  and  $D_F$ , under the constraint  $\sum_{n=0}^{M_s-1} c_n^2 = 1$ . As shown in Fig. 2(a), for a fixed  $D_F$ , QFI increases with  $M_s$  up to a saturation value of  $M_s^{\max} \approx \sqrt{2D_F}$  (see Ref. [25]). Beyond this value, as visualized in Fig. 2(b) (dashed blue), the maximum QFI scales roughly as  $K_{\max} \approx 13.2D_F^{1.1}$  for  $D_F \in (0, 100]$ , corresponding to a (normalized) displacement imprecision lower bound of

$$\Delta\tilde{d} \gtrsim \frac{1}{3.6\sqrt{D_F^{1.1}N}}. \quad (9)$$

The bound in Eq. (9) is the quantum Cramér-Rao bound [15] (QCRB) for transverse beam-displacement sensing through a matched pair of Gaussian apertures. For comparison, inserting  $(c_0, \theta_0) = (1, 0)$  into Eq. (8) yields the optimum displacement precision for a conventional  $\text{HG}_{00}$  coherent state transmitter

$$\Delta\tilde{d}_{00} \geq \frac{\sqrt{D_F/2}}{\sqrt{(\sqrt{1+4D_F}-1)^3N}} \approx \frac{1}{4\sqrt{D_F^{0.5}N}}. \quad (10)$$

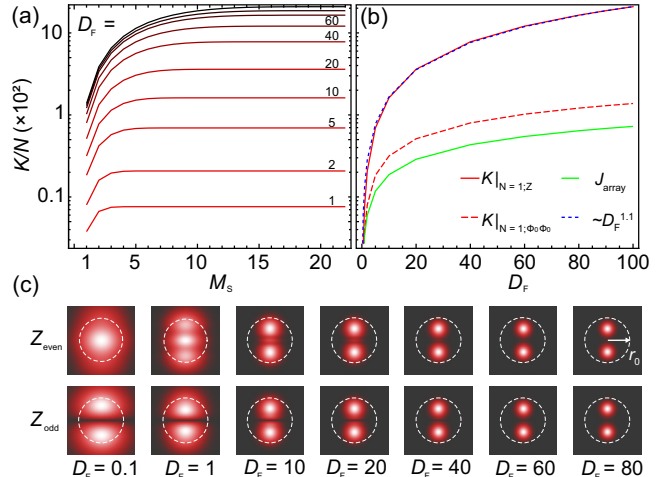


FIG. 2. (a) Displacement QFI ( $K$ ) versus modal support ( $M_s$ ) for optical systems with different Fresnel-number product ( $D_F$ ), normalized to the mean photon number  $N$  of the transmitter. (b) QFI versus  $D_F$  for a transmitter in the fundamental  $\text{HG}_{00}$  mode (dashed red) and an optimum spatial mode (solid red). Green is the CFI for the array-based transceiver in Table I. Blue is a power-law fit,  $13.2D_F^{1.1}$ . (c) Even  $Z_{\text{even}}$  ( $M_s \in 2\mathbb{Z}$ ) and odd  $Z_{\text{odd}}$  optimal modes for different  $D_F$ . Any optimal mode can be written as superposition of  $Z_{\text{even}}$  and  $Z_{\text{odd}}$ .

Evidently  $\Delta\tilde{d}_{00}/\Delta\tilde{d} \approx D_F^{0.3}$  for  $D_F \in (0, 100]$ , which implies that a tenfold reduction in mean squared error is possible, by mode-shape engineering, at  $D_F = 100$ .

In order to take advantage of the scaling in Eq. (9), it is necessary to use an optimal spatial mode shape and receiver. In Fig. 2(c), we present classically optimal transmitter spatial modes  $Z(x, y)$  for various  $D_F$ , determined by maximizing Eq. (8) over  $\{c_n, \theta_n\}$  for a modal support  $M_s$  high enough to saturate the QFI, as shown in Fig. 2(a). Evidently  $Z$  exhibits a bimodal intensity distribution along the displacement ( $x$ ) direction, whose root-mean-square distance from the optical axis increases with the aperture size  $r_0$ . Not shown is the phase profile of the mode, which exhibits rapid oscillations within the intensity envelope with a period approximately  $r_0/\sqrt{D_F}$ . These oscillations account for the high spatial frequency content of the modeshape, and are practical considerations for receiver architectures at high  $D_F$ , as discussed below.

We now turn our attention to the identification of optimal receivers, using CFI ( $J$ ) as a figure of merit. Formally, for a specific measurement applied to a displaced laser beam

$$J(\tilde{d}) = \int \left( \frac{\partial P(\vec{\gamma}; \tilde{d})}{\partial \tilde{d}} \right)^2 \frac{1}{P(\vec{\gamma}; \tilde{d})} d\vec{\gamma}, \quad (11)$$

where  $P(\vec{\gamma}; \tilde{d})$  is the probability of measurement outcome  $\vec{\gamma}$  given normalized displacement  $\tilde{d}$ . To identify an optimal receiver for a given transmitter mode, we demand

that it satisfy the upper bound  $J(\tilde{d}) = K(\tilde{d})$  in Eq. (1), which corresponds to an optimal displacement imprecision  $\Delta\tilde{d} = 1/\sqrt{J(\tilde{d})}$  saturating the QCRB given in Eq. (9). (We note that for single parameter estimation, the existence of such an optimal receiver is assured [15].)

We focus on optimal receiver designs for a coherent state transmitter in an odd-ordered optimal spatial mode  $Z(x, y)$  (subscript omitted), shown in Fig. 2(c). After propagation, it is convenient to express the received field in the form

$$\begin{aligned} \psi &= \sqrt{N} \sqrt{\eta_Z} \zeta_0(x + d, y) A_d(x, y) \\ &\approx \sqrt{N} \left( \sum_{n=0}^{M_s/2-1} \alpha_{2n+1} \eta^{n+1} e^{in\pi/2} \phi_{2n+1}(x), \right. \\ &\quad \left. + \tilde{d} \sum_{n=0}^{M_s/2} \beta_{2n} e^{i(\vartheta_{2n} + \vartheta_0)} \phi_{2n}(x) \right) \phi_0(y), \\ &\equiv \sqrt{N} \sqrt{\eta_Z} \left( \zeta_0(x, y) + \sqrt{\beta} \tilde{d} \zeta_1(x, y) \right), \end{aligned} \quad (12)$$

where  $\{\zeta_0, \zeta_1\}$  form an orthonormal principal component basis for the receiver and  $A_d = e^{(d^2+2xd)/r_R^2}$  is a correction factor for the displaced receiver aperture, and  $\alpha_n$  and  $\beta_n$  are expansion coefficients that optimize Eq. (8) [24]. If there is no displacement, photons in transmitter mode  $Z$  will occupy mode  $\zeta_0$  at the receiver, with a transmissivity  $\eta_Z$ . Displacement will cause photons to populate mode  $\zeta_1$  with coupling strength  $\beta$ . (In the Supplemental Material [24] we show that  $\eta_Z \beta = \sum_{n=0}^{M_s/2} \beta_{2n}^2$ , which, as shown in Fig. 2, can be approximated as  $\eta_Z \beta \approx 3.3 D_F^{1.1}$ .)

For sufficiently small beam displacement  $d$ , Eq. (12) implies that  $d$  is fully encoded in the complex amplitude of mode  $\zeta_1$ , and that, therefore, the optimal receiver design is independent of the magnitude of  $d$ . Since  $d$  is encoded in a phase-space displacement of  $\zeta_1$  [23], it can be shown that a homodyne receiver with its local oscillator (LO) in the  $\zeta_1$  mode is optimal [31]. When only the absolute displacement magnitude  $|d|$  is of interest, then phase-insensitive mode-sorting-based receivers are also optimal. In general, homodyne and SPADE are examples of a broader class of optimal receivers whose defining characteristic is the ability to resolve  $\zeta_1$  from  $\zeta_0$ .

In Fig. 3 we illustrate the concept of spatial-mode demultiplexing (SPADE) and “structured-LO” homodyning, representing two broad classes of optimal coherent state receivers for transverse beam displacement. A more detailed list is given in Table I, together with the traditional, suboptimal approach based on direct detection with a pixel array (DD-ARRAY). Below, we elaborate on the CFI analysis of SPADE, structured homodyne, and DD-ARRAY receivers, and under what circumstances they can be optimal.

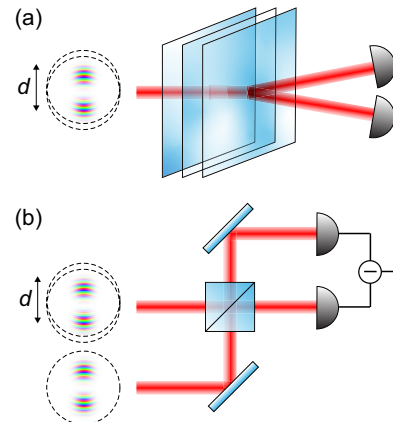


FIG. 3. Two optimal receivers for transverse beam displacement: (a) a spatial mode sorter, which has been configured to distill the optimal transmitter mode  $Z$  from its orthogonal complement, and (b) a homodyne interferometer with a local oscillator in the  $\zeta_1$  mode.

For simplicity, we first consider the structured homodyne receiver illustrated in Fig. 3(b). By interfering the received field with a LO in the information-carrying  $\zeta_1$  mode, an appropriate LO phase yields a (real) quadrature estimate with mean  $\langle \hat{q} \rangle = \sqrt{4\eta_Z N \beta \tilde{d}}$  and variance  $\langle \Delta \hat{q} \rangle = 1$  [23], corresponding to

$$J_{\text{hom}}(\tilde{d}) = 4\eta_Z N \beta. \quad (13)$$

Rewriting Eq. (8) in the principal-component basis  $\{\zeta_0, \zeta_1\}$ , it is straightforward to show that  $J(\tilde{d}) = K(\tilde{d})$  [24], implying that structured homodyne is indeed an optimal receiver.

For the SPADE receiver [Fig. 3(a)], the displaced beam is passed through a series of phase plates that sort principal-component modes  $\zeta_0$  and  $\zeta_1$  into different paths. (Mode sorting in the HG and other orthonormal bases has been widely realized [26–28]; we here consider a reconfigurable mode sorter [29].) Direct photon counting is then carried out in the  $\zeta_1$  beam path. The set of possible counts  $\{n_1\}$  follows a Poisson distribution with mean value  $N_1 = \eta_Z N \beta \tilde{d}^2$ , yielding a CFI

$$J_{\text{SPADE}}(\tilde{d}) = \sum_{n_1=0}^{\infty} \left( \frac{\partial P(n_1; \tilde{d})}{\partial \tilde{d}} \right)^2 \frac{1}{P} = \left( \frac{\partial N_1}{\partial \tilde{d}} \right)^2 \frac{1}{N_1}, \quad (14)$$

TABLE I. Classical transceiver designs and their optimality.

Transmitter	Receiver	CFI attaining?
$Z(x)\Phi_0(y)$	HGSPADE-DD [26–28]	Yes
$Z(x)\Phi_0(y)$	$\zeta$ -SPADE-DD [29]	Yes
$Z(x)\Phi_0(y)$	HGSPADE-homodyne [12]	Yes
$Z(x)\Phi_0(y)$	$\zeta$ -homodyne [24]	Yes
$\Phi_0(x)\Phi_0(y)$	HGSPADE-DD [26–28]	Yes
$\Phi_0(x)\Phi_0(y)$	ARRAY-DD [30]	No

where  $P(n_1; \tilde{d})$  is the conditional probability of  $n_1$  counts. It follows from the right-hand side of Eq. (14) that

$$J_{\text{SPADEF}}(\tilde{d}) = 4\eta_Z N \beta, \quad (15)$$

implying that SPADE in the  $\{\zeta_0, \zeta_1\}$  basis, together with direct photon counting of the  $\zeta_1$ -sorted light, is also an optimal receiver. In Ref. [24], we show that SPADE in the HG mode basis, followed by direct photon counting or homodyne of each output, is also optimal (HGSPADEF-DD and HGSPADEF-homodyne in Table I, respectively).

Finally, as an example of a nonideal receiver, we consider a traditional pixel array detector together with photon counting at each pixel. Pixel array detectors have been studied extensively for transverse beam-displacement sensing with both classical and squeezed light [5–8, 30, 32] (including split photodetection, which corresponds to a  $1 \times 2$  pixel array [5–8]). Following the typical case, we assume the transmitter is a coherent state in the  $\text{HG}_{00}$  mode. For simplicity, we also assume that the pixels are infinitesimally small with 100% fill factor [30, 32]. The output of this receiver is an infinite set of Poisson distributed random variables with mean  $\sigma_N(x, y, \tilde{d}) dx dy$ , where

$$\sigma_N(x, y, \tilde{d}) = N\eta|\phi_0(x + \tilde{d}r_R)\phi_0(y)A_d(x, y)|^2 \quad (16)$$

is the mean count density. Generalizing Eq. (14) then yields

$$J_{\text{array}}(\tilde{d}) = \iint \left( \frac{\partial \sigma_N}{\partial \tilde{d}} \right)^2 \frac{1}{\sigma_N} dx dy = 4\eta N \frac{(\sqrt{1 + 4D_F} - 1)^2}{\sqrt{1 + 4D_F}}, \quad (17)$$

where the integral is over all space.

We conclude by discussing the dynamic range of the receivers in Table I, particularly those employing an optimal transmitter mode  $Z$  with large modal support  $M_s \gg 1$ , whose characteristic length scale, approximately  $r_0/M_s$ , can be much smaller than the receiver aperture (cf. Fig. 3). In this case, the small displacement approximation  $\tilde{d} \ll 1$  underpinning Eq. (12) may be inappropriate, manifesting as a receiver-specific bias error  $\Delta\tilde{d}_{\text{bias}}$  that increases the total measurement error to

$$\Delta\tilde{d}_{\text{tot}} = \sqrt{\Delta\tilde{d}^2 + \Delta\tilde{d}_{\text{bias}}^2}. \quad (18)$$

In Fig. 4, we present Monte Carlo simulations of total error  $\Delta\tilde{d}_{\text{tot}}$  for transceivers employing pixel array and SPADE receivers with  $\text{HG}_{00}$  and  $Z$ -mode coherent state transmitters. (Homodyne and SPADE suffer similar dynamic range limitations; we focus on SPADE because of its simpler extension to different mode bases.) Specifically, we compare the canonical two-pixel split photodiode (SD)

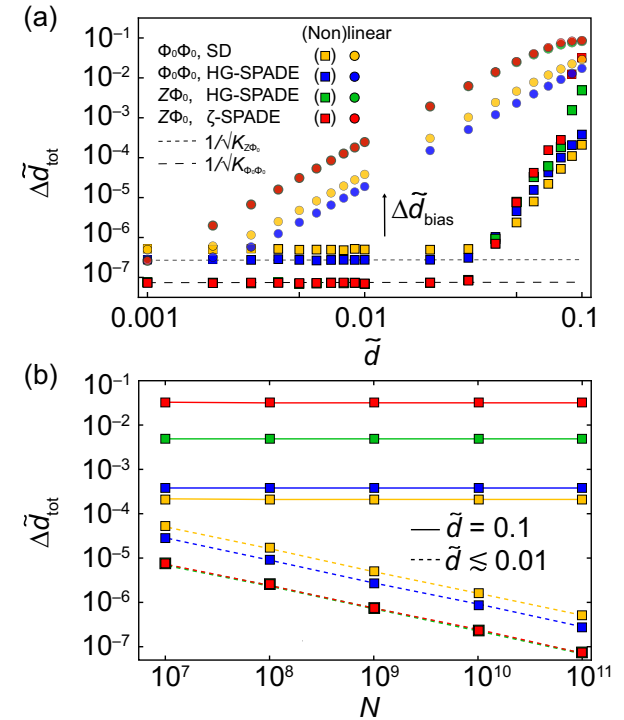


FIG. 4. (a) Simulated total measurement error versus actual displacement for various transceiver architectures, using linear and nonlinear estimators. (b) Simulated total measurement error versus photon number in the shot noise (dashed) and bias (solid) limited regime.

receiver to SPADE receivers employing an HG mode sorter [28] and a reconfigurable mode sorter in the  $\{\zeta_0, \zeta_1\}$  basis, for a system with  $D_F = 90$ . Based on the standard maximum-likelihood estimator, we devise a linear and nonlinear estimator for processing the receiver output (see the Supplemental Material [24]). As expected, we find that  $Z$ -mode transceivers have smaller imprecision  $\Delta\tilde{d}$  and higher bias error  $\Delta\tilde{d}_{\text{bias}}$  than  $\text{HG}_{00}$  transceivers; however, the bias error can be reduced using a nonlinear estimator (at the expense of computational overhead) yielding a total error that approaches the QCRB for  $\tilde{d} \leq 0.01$ , indicated by the black dashed lines in Fig. 4(a). We emphasize that the dynamic range—the displacement  $\tilde{d}$  at which  $\Delta\tilde{d}_{\text{bias}} = \Delta\tilde{d}$ —depends on both the measurement strength  $N$  and the estimation strategy, and can, in principle, be extended for more optimal estimators, as well as by active stabilization of the beam position.

In summary, we have used quantum Fisher information to design an optimal transceiver for laser beam-displacement sensing. Assuming the probe is in a coherent state and modeling propagation loss as a pair of Gaussian apertures at the transmitter (laser) and receiver, we find that the optimal spatial mode is a bimodal distribution (Fig. 2) that balances the trade-off between maximizing

spatial frequency content and minimizing aperture loss. We emphasize that this spatial mode is optimized over all degrees of freedom of an optical system, including possible receivers, and is parameterized only by the system's Fresnel-number product  $D_F$ . Its mean-squared error relative to the traditional fundamental Gaussian mode transceiver scales as approximately  $D_F^{0.6}$ , yielding a ten-fold improvement for practically relevant  $D_F \sim 100$ . We also studied various receiver architectures, using classical Fisher information as a metric, and showed that homodyne and SPADE receivers can each extract maximal information (CFI = QFI) about beam displacement when appropriately tailored to the transmitter mode (Fig. 3), while traditional pixel array receivers cannot. Finally, we considered the dynamic range of SPADE and two-pixel (split detector) receivers, and showed that the increased bias error inherent to the optimal spatial mode can, in principle, be reduced with a nonlinear estimator (Fig. 4).

Looking forward, we emphasize that our results are both practically relevant, given recent rapid advances in structured light preparation [17], and extensible to nonclassical probe states, such as squeezed light. Combining these two resources—spatial mode structuring and squeezing—can provide access to Heisenberg scaling  $\Delta d \sim 1/N$  [33,34] for beam-displacement measurements and related imaging tasks (such as deflectometry), and has close connections to recent work in entanglement-enhanced distributed sensing [35,36], albeit with a fundamentally different set of challenges and applications related to the spatial-mode entanglement encoding.

*Acknowledgments.* W.H. and S.G. acknowledge Office of Naval Research (ONR) Contract No. N00014-19-1-2189, and Air Force Office of Scientific Research (AFOSR) Contract No. FA9550-22-1-0180 for sponsoring this research. C.N.G. acknowledges funding support from the National Science Foundation, FET, Award No. 2122337. D.J.W. acknowledges support from the National Science Foundation through Award Nos. 2239735 and 2330310.

The authors declare no conflicts of interest.

- 
- [1] C. A. Putman, *et al.*, *J. Appl. Phys.* **72**, 6 (1992).
  - [2] M. A. Taylor, *et al.*, *Nat. Photonics* **7**, 229 (2013).
  - [3] Y. Kaymak, *et al.*, *IEEE Commun. Surv. Tutor.* **20**, 1104 (2018).
  - [4] M. D. Perrin, D. S. Acton, C.-P. Lajoie, J. S. Knight, M. D. Lallo, M. Allen, W. Baggett, E. Barker, T. Comeau, E. Coppock *et al.*, in *Space Telescopes and Instrumentation 2016: Optical, Infrared, and Millimeter Wave* (SPIE, Edinburgh, United Kingdom, 2016), Vol. 9904, p. 142.

- [5] C. Fabre, J. Fouet, and A. Maître, *Opt. Lett.* **25**, 76 (2000).
- [6] N. Treps, *et al.*, *Phys. Rev. Lett.* **88**, 203601 (2002).
- [7] N. Treps, *et al.*, *Science* **301**, 940 (2003).
- [8] E. Fradgley, *et al.*, *Opt. Express* **30**, 39374 (2022).
- [9] W. Larson and B. E. A. Saleh, *Phys. Rev. A* **102**, 013712 (2020).
- [10] V. Delaubert, *et al.*, *Phys. Rev. A* **74**, 053823 (2006).
- [11] V. Delaubert, *et al.*, *Opt. Lett.* **31**, 1537 (2006).
- [12] H. Sun, *et al.*, *Appl. Phys. Lett.* **104**, 121908 (2014).
- [13] H. Qi, *et al.*, arXiv preprint [arXiv:1808.01302](https://arxiv.org/abs/1808.01302).
- [14] J. Shapiro, S. Guha, and B. Erkmen, *J. Opt. Netw.* **4**, 501 (2005).
- [15] S. L. Braunstein and C. M. Caves, *Phys. Rev. Lett.* **72**, 3439 (1994).
- [16] S. L. Braunstein, C. M. Caves, and G. J. Milburn, *Ann. Phys. (N. Y.)* **247**, 135 (1996).
- [17] C. Rosales-Guzmán and A. Forbes, *How to Shape Light with Spatial Light Modulators* (SPIE Press, Bellingham, Washington, 2017).
- [18] G. Lazarev, *et al.*, *Opt. Express* **27**, 16206 (2019).
- [19] C. L. Panuski, *et al.*, *Nat. Photonics* **16**, 834 (2022).
- [20] W. He, C. M. Pluchar, I. Ozer, A. Rubenok, D. J. Wilson, and S. Guha, in *Frontiers in Optics* (Optica Publishing Group, Tacoma, Washington United States, 2023), p. FTh3D-5.
- [21] H. L. Van Trees, *Detection, estimation, and modulation theory, Part I: Detection, estimation, and linear modulation theory* (John Wiley & Sons, 2004).
- [22] A. Uhlmann, The “transition probability” in the state space of  $a^*$ -algebra, *Rep. Math. Phys.* **9**, 273 (1976).
- [23] C. Weedbrook, *et al.*, *Rev. Mod. Phys.* **84**, 621 (2012).
- [24] See Supplemental Material at <http://link.aps.org/supplemental/10.1103/PhysRevApplied.22.L041004> for derivation of the cross-talk matrix, Fisher information analysis for Z-mode transceiver, and Monte Carlo simulation for dynamic range analysis.
- [25] The total number of HG modes with near unity transmissivity is approximately  $D_F$ . For the one-dimensional problem at hand we have approximately  $\sqrt{2D_F}$  HG modes with near unity transmissivity when keeping  $\Phi_0(y)$  as the mode function along the  $y$  axis.
- [26] N. K. Fontaine, *et al.*, *Nat. Commun.* **10**, 1 (2019).
- [27] Y. Zhou, *et al.*, *Opt. Lett.* **43**, 5263 (2018).
- [28] P. Boucher, *et al.*, *Optica* **7**, 1621 (2020).
- [29] I. Ozer, M. R. Grace, and S. Guha, in *2022 Conference on Lasers and Electro-Optics (CLEO)* (IEEE, San Jose, CA, USA, 2022), p. 1.
- [30] M. T. Hsu, *et al.*, *J. Opt. B: Quantum Semiclassical Opt.* **6**, 495 (2004).
- [31] C. Oh, *et al.*, *Phys. Rev. A* **100**, 012323 (2019).
- [32] J. Chao, E. S. Ward, and R. J. Ober, *JOSA A* **33**, B36 (2016).
- [33] V. Giovannetti, S. Lloyd, and L. Maccone, *Phys. Rev. Lett.* **96**, 010401 (2006).
- [34] M. Gessner, N. Treps, and C. Fabre, *Optica* **10**, 996 (2023).
- [35] Y. Xia, *et al.*, *Nat. Photonics* **17**, 1 (2023).
- [36] M. R. Grace, C. N. Gagatsos, and S. Guha, *Phys. Rev. Res.* **3**, 033114 (2021).